Q-switching pulse generation using black phosphorus tape saturable absorber

HARITH AHMAD[a], NOR AHYA HASSAN[a], SITI NABILA AIDIT[a], SHOK ING OOI[a], SULAIMAN WADI HARUN[b], ZIAN CHEAK TIU[*]
[a]*Photonics Research Center, University of Malaya, 50603 Kuala Lumpur, Malaysia*
[b]*Department of Electrical Engineering, Faculty of Engineering, University of Malaya 50603 Kuala Lumpur, Malaysia*

Passive Q-switched Erbium-doped fiber laser (EDFL) and Ytterbium-doped fiber laser (YDFL) incorporating black phosphorus (BP) tape as saturable absorber is proposed and practically demonstrated. A clean tape is used to mechanically exfoliate few layers BP from 99.995% purity BP crystal. The BP tape is cut into a small piece and sandwiched between two standard FC/PC fiber ferrule end surfaces with index matching gel. Q-switching operation of EDFL and YDFL is occurred between pump power range of 35.7 mW to 115.5 mW and 115.2 mW to 188.0 mW respectively.

(Received March 25, 2016; accepted February 10, 2017)

Keywords: Q-switched, Black phosphorus, Fiber laser

Q-switched fiber lasers are very efficient in generating high energy pulses at low repetition rates and are widely used in versatile fields such as material processing, remote sensing, micromachining, telecommunications, medicine, fiber sensing, and range finding [1- 3]. There have been many reports of Q-switching fiber lasers so far, which is either based on active or passive Q-switching. Active Q-switching uses an externally-modulated Q-switch, such as acousto-optic modulators [4] and electro-optic modulators [5], which allows for flexible repetition rate changes and timing synchronization. This method is rather expensive and mostly applicable in free space. Passively Q-switching method is a good alternative, as it is generally low cost, easier to fabricate and adaptable to fiber laser [1]. Passive Q-switching operation has been successfully demonstrated using various SAs previously. Semiconductor saturable absorber mirror (SESAM) have had short success stint as the SA of choice. SESAMs mostly operate at single wavelength [6]. Its shortcomings include expensive fabrication cost, and prone to be easily damaged when exposed to Q-switching instabilities. Due to its limitations, there emerged a need to explore other alternatives, and carbon nanotube (CNT) provided this [7, 8]. But CNT had limitations too, where its operating wavelength is highly dependent on the core diameter of CNT.

Consequently, there have been interest to explore other materials that can provide broader operating wavelength range. Of recent, following the discovery of graphene in 2004 [9], there have been demonstrations of using graphene as SA to generate short pulses in fiber lasers [10 – 19]. Subsequently, many works on Q switching had been reported. Graphene's limitation is that it has low modulation depth, and this has induced researchers to explore other 2D materials such as transition metal dichalcogenides (TMD) and topological insulator (TI). TMD group form layered structures in the form of X-M-X, where two chalcogen atoms planes sandwich a metal atoms plane. An example of TMD that has garnered interest lately is Molybdenum Disulfide (MoS_2). The saturable absorption property in MoS_2 has been reported to be better than graphene [20]. There have been many reports on Q-switching fiber lasers using TMDs [21 – 23]. On the other hand, TIs possess bulk bandgap like ordinary insulators and a protected conducting state on their edges or surface [24–27], which provide TIs with broadband nonlinear optical response [28]. There have been many reports on Q-switching fiber lasers using TI as well [29 – 31].

Meanwhile, Black Phosphorus (BP) is another emerging material that has recently joined in the family of 2D materials [32-34]. BP possess layer dependent direct bandgap. Its bandgap increases with the decrease of the thickness, from 0.3 eV (bulk) to 1.5 eV (monolayer) [35 - 37]. The basic structure of BP is similar to bulk graphite, where individual atomic layers are stacked together by van der Waals forces. [38]. Inside the single layer, each phosphorus atom is covalently bonded with three adjacent phosphorus atoms and form a puckered honeycomb structure. Arising from this, very recently there have also been initial work of using BP as SA, which can be fabricated using liquid phase exfoliation (LPE) or mechanical exfoliation (ME). Lu et. al, demonstrated LPE as a means to produce a BP SA, where his experiment highlights BP as a possible candidate for Q switching and mode locking [39]. Besides that, Haoran Mu has demonstrated sandwiched PMMA-BP-PMMA membrane as saturable absorber to induce Q-switching operation [40]. These methods show promising results in Q-switched fiber laser. However, these methods involve complicated chemical works and costly equipments to fabricate the BP SA. Meanwhile, there are reported works that use mechanical exfoliation method as well to fabricate BP as

SA. Mechanical exfoliation is advantageous with its simplicity, where the entire fabrication process does not involve any complicated chemical procedure and costly instruments. Thin flakes are peeled off repeatedly from crystals using adhesive tape. This exfoliation method provides advantages such as low cost, uniformity, and ease of fabrication. By using mechanically exfoliated BP as saturable absorber, Diao Li has demonstrated the generation of Q-switched fiber laser [41]. Tian Jiang also demonstrated Q switched pulse lasers operating at 1550 nm and 2 μm wavelengths [42]. Yu Chen demonstrated Q-switching and mode-locking pulsed lasers. [43]. In all these three works thin flakes are peeled off repeatedly from crystals nd then are attached to standard FC/PC fiber ferrules.

In this paper, a passive Q-switch fiber laser working in the 1550 nm region and 1060 nm region is demonstrated. The BP tape SA was prepared by mechanical exfoliation method. The novelty in our work lies in the fact that we attached a small piece of BP tape SA to standard FC/PC fiber ferrules. This method, although simple and easy, is a viable alternative to the methods previously used.

As shown in Fig. 1, relatively thin flakes from a commercially available 99.995% purity BP crystal (HQGraphene) were placed on a clear adhesive tape, or more popularly known as scotch tape. Then, the flakes adhered on the scotch tape were pressed so that they become uniformly spread throughout the tape. After that, a small portion of the tape with BP flakes were cut and attached to a standard FC/PC fiber ferrule ending to the side with BP flakes. The other side of the tape is connected to another standard FC/PC fiber ferrule. In short, the BP tape is sandwiched between two standard FC/PC fiber ferrule end surfaces with index matching gel.

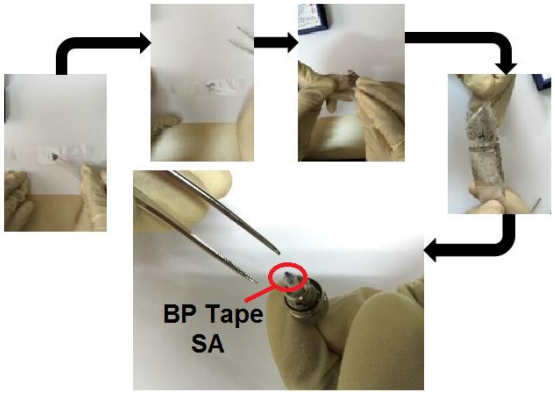

Fig. 1. Mechanical exfoliation method showing BP thin flakes placed on a clear scotch tape, pressed, and subsequently a small piece of the tape was cut and placed on a standard FC/PC fiber ferrule

The BP tape is investigated with Raman spectroscopy. Fig. 2 shows the Raman spectrum, which is recorded by a spectrometer when a 514 nm beam of a He-Ne laser is radiated onto the tape for 10 ms with an exposure power of 10 mW. As shown in the figure, the sample exhibits three distinct Raman peaks at 360 cm^{-1}, 438 cm^{-1} and 465 cm^{-1}, corresponding to the A_g^1, B_{2g} and A_g^2 vibration modes of layered BP. While the B_{2g} and A_g^2 modes correspond to the in-plane oscillation of phosphorus atoms in BP layer, the A_g^1 mode corresponds to the out-of-plane vibration. Other analysis of the SA such as FESAM, EDS, and nonlinear absorption behavior is elaborated in our previous work [44].

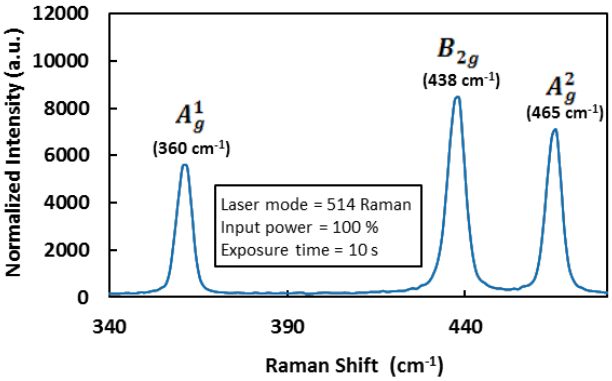

Fig. 2. Raman spectrum of the BP tape SA

The experimental set-up of the proposed Q-switched EDFL is illustrated in Fig. 3, which the ring resonator consists of a 3 m long Erbium-doped fiber (EDF) as the gain medium, 980/1550 nm wavelength division multiplexer (WDM), Isolator, 3 dB output coupler (OC1), and BP tape SA.. A 980 nm laser diode is used to pump the EDF via the WDM. An isolator is placed in the cavity to ensure the unidirectional light propagation in the cavity. The BP tape SA is cut into a small piece and sanwiched between two standard FC/PC fiber ferrule end surface with index matching gel. The laser light is extracted from the cavity by OC1 coupler which retains 50% of the light in the cavity for further oscillation. An optical spectrum analyzer (OSA) with wavelength resolution of 0.02 nm is used to capture the output laser spectrum while a 500 MHz oscilloscope in conjunction with 1.2 GHz bandwidth photo-detector is used to detect the pulse train.

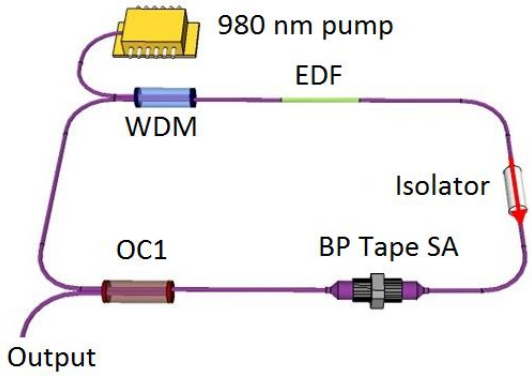

Fig. 3. Schematic diagram of the proposed Q-switched EDFL

The oscillator started the Q-switching operation after reaching the launched pump power of 35.7 mW. The Q-switching operation occured with pump power range up to 115.5 mW. Stable self-starting Q-switched pulses were observed as shown in Fig. 4 from pump power of 35.7 mW to 115.5 mW. However, as the pump power further increases, the pulse train becomes unstable and disappears. As shown in Fig. 4, the pulse duration reduces whereas the pulse amplitude increases as the pump power increases within the Q-switching operation range. The SNR of 52 dB at frequency of 31 kHz indicated the stability of the Q-switching operation at threshold pump power, as shown in inset of Fig. 4. Fig. 5 shows the output spectra of the EDFL when the pump power is fixed at 115.5 mW. The Q-switching operation of the proposed EDFL is centered at 1563.7 nm.

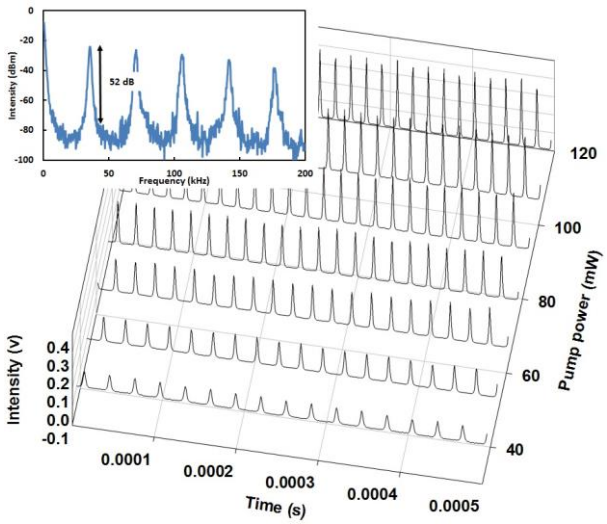

Fig. 4. Q-switched pulse evolution of the proposed Q-switched EDFL against pump power. Inset is RF spectrum of Q-switching operation at threshold pump power

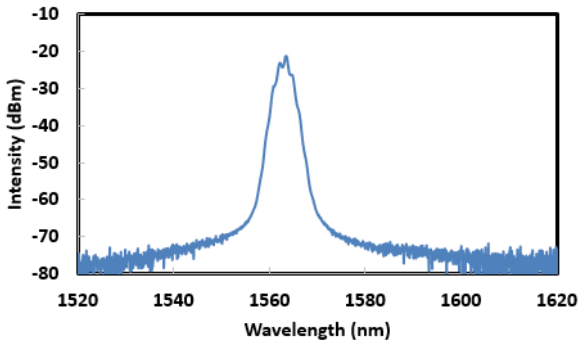

Fig. 5. Optical spectrum of the proposed Q-switched EDFL when the pump is fixed at 115.5 mW

Fig. 6 shows the relationship of repetition rate and pulse width to the pump power. The pulse repetition rate can be seen to increase almost linearly with the increase of pump power. On the other hand, the pulse width decreases almost linearly with the increase of pump power. By pumping higher power into the cavity, it will increase the gain population excitation process to achieve the saturation state in BP SA. Thus, more pulses with narrower pulse width can be generated in a same period of time. This observation agrees well with the passively Q-switching theory. The pulse repetition rate of the Q-switched EDFL can be tuned from 31.5 kHz to 46.8 kHz by varying the pump power from 35.7 mW to 115.5 mW. Besides, the pulse width reduces from 31.74 µs to 21.3 µs as the pump power increases in the range of Q-switching operation.

The average output power of the proposed Q-switched EDFL is measured and applied to the calculation of the corresponding single-pulse energy. Fig. 7 shows the relationship of average output power and pulse energy of the Q-switched EDFL against pump power. As shown in the figure, average output power almost linearly increased from 0.6 mW to 2.1 mW as the pump power increases from 35.7 mW to 115.5 mW. In the range of Q-switching operation, the cavity efficiency is around 1.88% Besides, pulse energy exhibited increasing trend from 19.0 nJ to 44.9 nJ at the same pump power range.

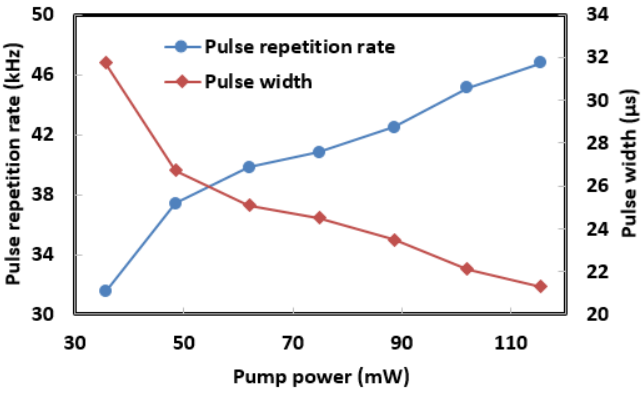

Fig. 6. Repetition rate and pulse width of the proposed Q-switched EDFL against the pump power

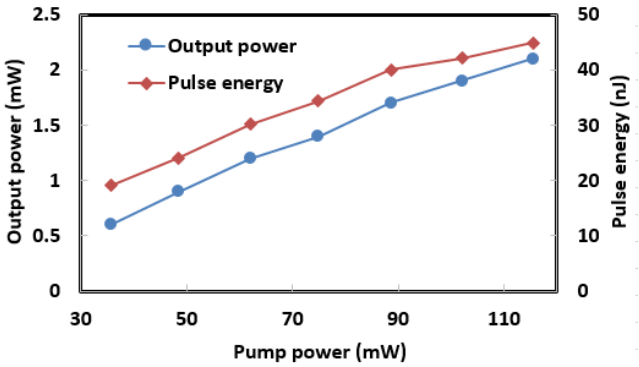

Fig. 7. Output power and pulse energy of the proposed Q-switched EDFL against the pump power

Next, the BP SA is insert into a 1 micron cavity as shown in Fig. 8. The experimental set-up is similar to EDFL, but the gain medium and WDM are changed to Ytterbium-doped fiber (YDF) and 980/1060 nm WDM respectively. The wavelength of the Q-switched YDFL is centered at 1036 nm as shown in Fig. 9.

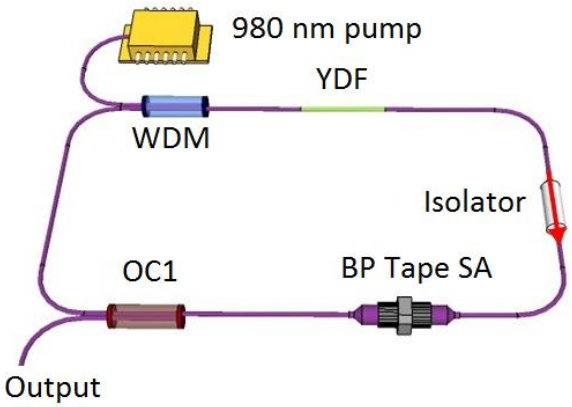

Fig. 8. Schematic diagram of the proposed Q-switched YDFL

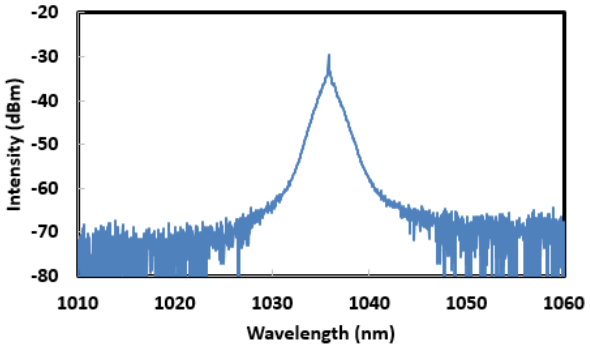

Fig. 9. Optical spectrum of the proposed Q-switched YDFL when the pump is fixed at 115.5 mW

The Q-switching occured within the pump power range from 115.2 mW to 188.0 mW as shown in Fig. 10. The time interval between pulse reduces while the pulse amplitude increases as the pump power increases within the Q-switching operation range. The SNR of 57 dB at frequency of 45 kHz presented the stability of the Q-switching operation at threshold pump power, as shown in inset of Fig. 10. Fig. 11 shows how repetition rate and pulse width are related to the pump power. The pulse repetition rate of the Q-switched YDFL can be tuned from 45.0 kHz to 71.7 kHz by varying the pump power from 115.2 mW to 188.0 mW. On the other hand, the pulse width reduces from 22.2 μs to 13.9 μs as the pump power increases in the range of Q-switching operation. The average output power is measured and applied to the calculation of the corresponding single-pulse energy. Fig. 12 shows the relationship of average output power and pulse energy of the Q-switched YDFL against pump power. As shown in the figure, average output power almost linearly increased from 0.11 mW to 0.22 mW as the pump power increases from 115.2 mW to 188.0 mW. Besides, pulse energy exhibited increasing trend from 2.4 nJ to 3.0 nJ at the same pump power range.

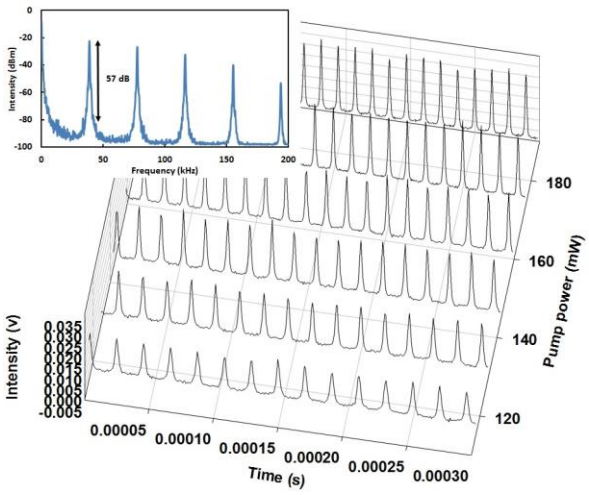

Fig. 10. Q-switched pulse evolution of the proposed Q-switched YDFL against pump power. Inset is RF spectrum of Q-switching operation at threshold pump power

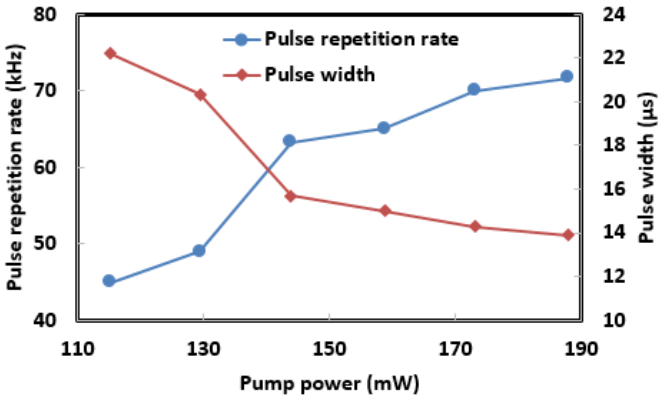

Fig. 11. Repetition rate and pulse width of the proposed Q-switched YDFL against the pump power

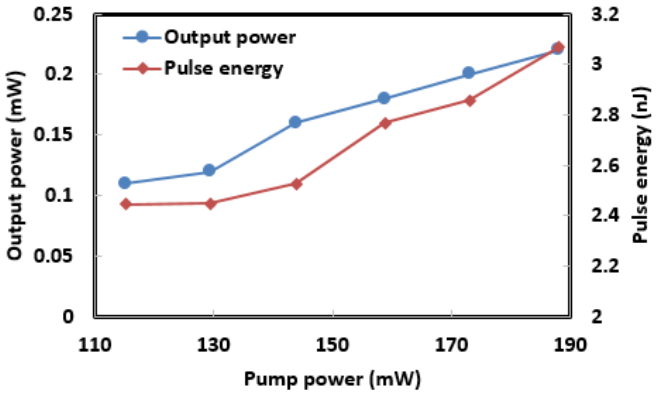

Fig. 12. Output power and pulse energy of the proposed Q-switched YDFL against the pump power

Overall, the BP tape SA performed similar function to other TMD [21-23, 45-46] and graphene based SA [20]. However, BP based SA provide different set of characteristic, which could be an alternative solution as optical material.

In conclusion, we have proposed and practically demonstrated the passive Q-switched EDFL and YDFL laser with an incorporation of BP tape as saturable absorber. A clean tape is used to mechanically exfoliate few layer BP from 99.995% purity BP crystal. The BP tape is cut into a small piece and sandwiched between two standard FC/PC fiber ferrule end surfaces with index matching gel. Q-switching operation of EDFL and YDFL is occurred between pump power range of 35.7 mW to 115.5 mW and 115.2 mW to 188.0 mW respectively. The highest pulse energy obtained in EDFL and YDFL is 44.9 nJ and 3.0 nJ respectively.

Acknowledgement

We would like to acknowledge the generous funding from University of Malaya through the grant UM.C/625/1/HIR/MOHE/SCI/29 and also from LRGS(2015)/NGOD/UM/KPT

References

[1] R. Paschotta, R. Häring, E. Gini, H. Melchior, U. Keller, H. L. Offerhaus, D. J. Richardson, Opt. Lett. **24**(6), 388 (1999).
[2] T. Hakulinen, O. G. Okhotnikov, Opt. Lett. **32**(18), 2677 (2007).
[3] R. R. Gattass, E. Mazur, Nat. Photonics **2**(4), 219 (2008).
[4] Z. J. Chen, A. B. Grudinin, J. Porta, J. D. Minelly, Opt. Lett. **23**(6), 454 (1998).
[5] A. F. El-Sherif, T. A. King, Opt. Commun. **218**(4–6), 337 (2003).
[6] U. Keller, K. J. Weingarten, F. X. Kärtner, D. Kopf, B. Braun, I. D. Jung, J. A. D. Au, IEEE Journal of Selected Topics in Quantum Electronics **2**(3), 435 (1996).
[7] D.-P. Zhou, L. Wei, B. Dong, W.-K. Liu, IEEE Photon. Technol. Lett. **22**, 9 (2010).
[8] S. Yamashita, Y. Inoue, et al., Opt. Lett. **29**(14), 1581 (2004).
[9] K. S. Novoselov, A. K. Geim, S. V. Morozov, D. Jiang, Y. Zhang, S. V. Dubonos, I. V. Grigorieva, V. V. Firsov, Science **306**(5696), 666 (2004).
[10] Q. Bao, H. Zhang, et al., Advanced Functional Materials **19**(19), 3077 (2009).
[11] T. Hasan, Z. Sun, et al., Adv. Mater. **21**(38-39), 3874 (2009).
[12] L. Zhang, J. T. Fan, J. H. Wang, J. M. Hu, M. Lotya, G. Z. Wang, Y. Feng, Laser Physics Letters **9**(12), 888 (2012).
[13] J. Liu, S. Wu, Q. H. Yang, P. Wang, Opt. Lett. **36**, 4008 (2011).
[14] Z. Q. Luo, M. Zhou, J. Weng, G. Huang, H. Xu, C. Ye, Z. P. Cai, Opt. Lett. **35**, 3709 (2010).
[15] G. Sobon, J. Sotor, J. Jagiello, R. Kozinski, K. Librant, M. Zdrojek, L. Lipinska, K. M. Abramski, Appl. Phys. Lett. **101**, 241106 (2012).
[16] M. A. Ismail, F. Ahmad, S. W. Harun, H. Arof, H. Ahmad, Laser Physics Letters **10**(2), 025102 (2013).
[17] D. Popa, Z. Sun, T. Hasan, F. Torrisi, F. Wang, A. C. Ferrari, Appl. Phys. Lett. **98**(7), 073106 (2011).
[18] W. Li, Z. Da-Peng, H. Y. Fan, L. Wing-Ki, Photonics Technology Letters, IEEE **24**(4), 309 (2012).
[19] Z. Junqing, Y. Peiguang, R. Shuangchen, Y. Yongqin, D. Geguo, Z. Gelin, L. Jie, Optical Engineering **51**(7), 074201 (2012).
[20] K. Wang, J. Wang, J. Fan, M. Lotya, A. O'Neill, D. Fox, Q. Zhao, ACS Nano, **7**(10), 9260 (2013).
[21] Z. Luo, Y. Huang, M. Zhong, Y. Li, J. Wu, B. Xu, J. Weng, Journal of Lightwave Technology **32**(24), 4077 (2014).
[22] R. Woodward, E. Kelleher, R. Howe, G. Hu, F. Torrisi, T. Hasan, J. Taylor, Opt. Express **22**(25), 31113(2014).
[23] H. Li, H. Xia, et al., Photonics Technology Letters IEEE **27**(1), 69v (2015).
[24] H. J. Zhang, C. X. Liu, X. L. Qi, X. Dai, Z. Fang, S.C. Zhang, Nat. Phys. **5**(6), 438 (2009).
[25] J. E. Moore, Nature **464**(7286), 194 (2010).
[26] D. Hsieh, D. Qian, L. Wray, Y. Xia, Y. S. Hor, R. J. Cava, M. Z. Hasan, Nature **452**(7190), 970 (2008).
[27] D. Hsieh, Y. Xia, D. Qian, L. Wray, J. H. Dil, F. Meier, J. Osterwalder, L. Patthey, J. G. Checkelsky, N. P. Ong, A. V. Fedorov, H. Lin, A. Bansil, D. Grauer, Y. S. Hor, R. J. Cava, M. Z. Hasan, Nature **460**(7259), 1101 (2009).
[28] S. Chen, C. Zhao, Y. Li, H. Huang, S. Lu, H. Zhang, S. Wen, Opt. Mater. Express **4**(4), 587 (2014).
[29] Y. Huang, Z. Luo, International Photonics and OptoElectronics Meetings, Wuhan, Optical Society of America (2014).
[30] Z. Yu, Y. Song, J. Tian, Z. Dou, H. Guoyu, K. Li, H. Li, X. Zhang, Opt. Express **22**, 11508 (2014).
[31] Z. Q. Luo, Y. Huang, J. Weng, H. Cheng, Z. Lin, B. Xu, Z. Cai, H. Xu, Opt. Express **21**, 29516 (2013).
[32] X. Zheng, R. Chen, G. Shi, J. Zhang, Z. Xu, T. Jiang, Opt. Lett. **40**(15), 3480 (2015).
[33] H. Yu, X. Zheng, K. Yin, T. Jiang, Optical Materials Express **6**(2), 603 (2016).
[34] R. Chen, Y. Tang, X. Zheng, T. Jiang, Applied Opt. **55**(36), 10307 (2016).
[35] L. Li, Y. Yu, G. J. Ye, Q. Ge, X. Ou, H. Wu, D. Feng, X. H. Chen, Y. Zhang, Nat. Nanotechnol. **9**(5), 372 (2014).
[36] H. Liu, A. T. Neal, Z. Zhu, Z. Luo, X. Xu, D. Tománek, P. D. Ye, ACS Nano **8**(4), 4033 (2014).
[37] V. Tran, R. Soklaski, Y. Liang, L. Yang, Phys. Rev. B **89**(23), 235319 (2014).
[38] H. Liu, Y. Du, Y. Deng, P. D. Ye, Chem. Soc. Rev. **44**(9), 2732 (2015).
[39] S. B. Lu, L. L. Miao, Z. N. Guo, X. Qi, C. J. Zhao, H.

Zhang, S. C. Wen, D. Y. Tang, D. Y. Fan, Opt. Express **23**(9), 11183 (2015).
[40] D. Li, H. Jussila, L. Karvonen, G. Ye, H. Lipsanen, X. Chen, Z. Sun, arXiv preprint, arXiv:1505.00480, (2015).
[41] H. Mu, S. Lin, Z. Wang, P. Li, Y. Chen, H. Zhang, H. Bao, S. P. Lau, C. Pan, D. Fan, Q. Bao, Advanced Optical Materials **3**(10), 1447 (2015).
[42] T. Jiang, K. Yin, X. Zheng, H. Yu, X. Cheng, arXiv preprint, arXiv:1504.07341, (2015).
[43] Y. Chen, G. Jiang, S. Chen, Z. Guo, X. Yu, C. Zhao, H. Zhang, Q. Bao, S. Wen, D. Tang, D. Fan, Opt. Express **23**(10), 12823 (2015).
[44] E. I. Ismail, N. A. Kadir, A. A. Latiff, H. Ahmad, S. W. Harun, RSC Advances **6**(76), 72692 (2016).
[45] H. Zhang, S. B. Lu, J. Zheng, J. Du, S. C. Wen, D. Y. Tang, K. P. Loh, Opt. Express **22**(6), 7249 (2014).
[46] J. Du, Q. Wang, G. Jiang, C. Xu, C. Zhao, Y. Xiang, Y. Chen, S. Wen, H. Zhang, Scientific reports **4** (2014).

*Corresponding author: zc_tiu@um.edu.my